European Journal of Pharmaceutics and Biopharmaceutics 77 (2011) 275–282

Contents lists available at ScienceDirect

European Journal of Pharmaceutics and Biopharmaceutics

journal homepage: www.elsevier.com/locate/ejpb

Research paper

Identification of permeability-related hurdles in oral delivery of curcumin using the Caco-2 cell model

Banrida Wahlang, Yogesh B. Pawar, Arvind K. Bansal *

Department of Pharmaceutics, National Institute of Pharmaceutical Education and Research (NIPER), Punjab, India

ARTICLE INFO

Article history:
Received 22 July 2010
Accepted in revised form 6 December 2010
Available online 13 December 2010

Keywords:
Curcumin
Caco-2 cells
Efflux
Permeability
Metabolism
Accumulation

ABSTRACT

Curcumin a poly-phenolic compound possesses diverse pharmacologic activities; however, its development as a drug has been severely impeded by extremely poor oral bioavailability. Poor aqueous solubility and extensive metabolism have been implicated for this but the role of membrane permeability has not been investigated. In the present study, permeability of curcumin was assessed using the Caco-2 cell line. Curcumin was poorly permeable with a P_{app} (A → B) value of $2.93 \pm 0.94 \times 10^{-6}$ cm/s. P_{app} value in (B → A) study was found out to be $2.55 \pm 0.02 \times 10^{-6}$ cm/s, thus ruling out the role of efflux pathways in poor oral bioavailability of curcumin. Studies using verapamil, a P-gp inhibitor, further confirmed this finding. Detailed mass balance studies showed loss of curcumin during transport. Further experiments using lysed cells revealed that 11.78% of curcumin was metabolized during transport. Studies using itraconazole, a CYP3A4 inhibitor, established its role in curcumin metabolism. Curcumin was also found to accumulate in cells as revealed by CLSM studies. Sorption and desorption kinetic studies further confirmed accumulation of curcumin inside the cells. Amount accumulated was quantitated by HPLC and found to be >20%. Thus, intestinal first-pass metabolism and intracellular accumulation played a role in poor permeability of curcumin. Based on its poor aqueous solubility and intestinal permeability, curcumin can be classified as a BCS Class IV molecule. This information can facilitate designing of drug delivery systems for enhancement of oral bioavailability of curcumin.

© 2010 Elsevier B.V. All rights reserved.

1. Introduction

Curcumin (CRM) also known as diferuloylmethane or curcumin I (CRM I) is the poly-phenolic compound obtained from the dried rhizomes of the dietary spice turmeric, i.e., *Curcuma longa*. Turmeric has been used in traditional Asian medicine like Ayurveda since time immemorial. CRM is regarded as the most active constituent of turmeric [1]. It was first characterized in 1910 by Lampe and Milobedzka [2] and is currently undergoing various stages of clinical trials for the treatment of numerous health disorders [3].

The above factors have triggered efforts to transform the 'CRM molecule' into a 'medicine'. Although the oral route of delivery is mostly preferred because of its safety, convenience and economy, CRM is a challenging molecule for this delivery route. A number of studies have been carried out to assess the bioavailability and pharmacokinetic properties of CRM in rodents [4] and humans [5].

Numerous challenges like poor aqueous solubility [6] and extensive metabolism lead to its poor systemic bioavailability. CRM has been found to have very poor absorption due to its poor aqueous solubility [7]. In clinical studies in healthy human volunteers, even after a dose of up to 4 g per day, negligible CRM levels were achieved in the plasma [8]. Oral administration of CRM in 12 patients with hepatic metastases showed that CRM was poorly available with extremely low levels of the parent compound present in the peripheral or portal circulation [9]. CRM undergoes extensive metabolic biotransformation during absorption via the gut and is subjected to a very high first-pass metabolism and possibly to enterohepatic recirculation [10–12]. Besides this, it has also been documented that CRM undergoes degradation in aqueous solution and at neutral and alkaline pH [13,14].

Aqueous solubility and intestinal permeability play a critical role in oral bioavailability of a compound. Suresh et al. assessed the absorption of CRM using the everted gut sac technique; however, the apparent permeability coefficient of the compound was not reported [15]. Moreover, the effect of pH was not assessed in the experiment, considering the stability of CRM at various pH conditions. Knowledge of the permeability value of CRM will facilitate classification of the compound according to the Biopharmaceutics Classification System (BCS).

The aim of the present work was to study the membrane permeability of CRM. Studies were conducted using the Caco-2 cell line which is a US FDA recommended method for determining the permeability of compounds [16].

* Corresponding author. Department of Pharmaceutics, National Institute of Pharmaceutical Education and Research (NIPER), S.A.S. Nagar, Mohali, Punjab 160 062, India. Tel.: +91 172 2214682 2126; fax: +91 172 2214692.
E-mail address: akbansal@niper.ac.in (A.K. Bansal).

0939-6411/$ - see front matter © 2010 Elsevier B.V. All rights reserved.
doi:10.1016/j.ejpb.2010.12.006

2. Materials and methods

2.1. Materials

Dulbecco's modified Eagle's medium (DMEM), hank's balanced salts solutions (HBSS), lucifer yellow (LY), 1α, 25-$(OH)_2$ vitamin D_3 and dimethyl sulfoxide (DMSO) were obtained from Sigma–Aldrich (Missouri, USA). Fetal bovine serum (FBS), heat inactivated, non-essential amino acids (NEAA) and trypsin–ethylenediamine tetra acetic acid (trypsin–EDTA) solutions were purchased from GIBCO, Invitrogen Corporation (New York, USA). Penicillin–Streptomycin–Amphotericin solution, 2-[4-(2-hydroxyethyl)-1-piperazinyl] ethanesulphonic acid (HEPES), 2-(N-morpholino) ethanesulphonic acid (MES), phosphate-buffered saline (PBS), 3-[4, 5-dimethylthiazol-2-yl]-2, 5-diphenyl tetrazolium bromide (MTT), sodium chloride and CRM were acquired from Himedia Laboratories Pvt. Ltd. (Mumbai, India). HPLC grade acetonitrile and methanol were obtained from J.T. Baker (Mexico City, Mexico) and tetrahydrofuran from Fischer Scientific (New Jersey, USA). Antipyrine (ANT) was purchased from Sigma–Aldrich (Missouri, USA), Furosemide (FSD), itraconazole and verapamil were a gift from IPCA Laboratories (Mumbai, India), Medicorp Technologies India Ltd. (Secunderabad, India) and Nicholas Piramal India Ltd. (Mumbai, India), respectively. Tris–HCl and ferrous sulfate were obtained from Loba Chemie Pvt. Ltd. (Mumbai, India). Citric acid monohydrate and zinc sulfate were purchased from Merck (Darmstadt, Germany) and absolute ethanol from Hong Yang Chemical Co. Ltd. (Jiangsu, China). Milli-Q grade water purified by a Milli-Q UV Purification System (Millipore, Massachusetts, USA) was used.

2.2. Methods

2.2.1. Cell culture

The Caco-2 cell line was obtained from American Type Culture Collection (ATCC, Virginia, USA) at passage no. 18. Cells were grown in DMEM supplemented with 15% of FBS, 1% Penicillin–Streptomycin–Amphotericin solution and 1% NEAA solution. Cells were cultured in T-75-cm^2 tissue culture flasks obtained from Cellstar®, Greiner Bio-One (Frickenhausen, Germany). The cell cultures were maintained at 37 °C in a CO_2 incubator, water jacketed with HEPA Class 100 (Forma Series II, Thermo electron Corporation, Ohio, USA). The incubator has an atmosphere of 95% air/5% CO_2 and 95% humidity. The cells became 80–85% confluent in 4–7 days after which they were harvested with trypsin–EDTA prior to seeding. The cells were grown on polycarbonate filters of 0.4 μm pore size (Millicell® 24-well Cell culture plate, Millipore, Massachusetts, USA) at a seeding density of 75,000 cells per well for 21–22 days to achieve a consistent monolayer. The growth media was changed, and the transepithelial electrical resistance (TEER) value was measured every alternate day. Cells from passage number 37–70 were used for the experiments.

2.2.2. 1α, 25-$(OH)_2$ vitamin D_3 treatment of Caco-2 cell monolayer

The Caco-2 cells were seeded on 24-well plates and grown for 10 days with supplemented DMEM mentioned in the previous section. After 10 days, the medium was additionally supplemented with zinc sulfate (3 nM), ferrous sulfate (5 nM) and 1α, 25-$(OH)_2$ vitamin D_3 (250 nM) [17]. The concentration of FBS was reduced to 5%, and the cells were maintained for another three weeks prior to the transport experiments.

2.2.3. MTT cytotoxicity assay

The cells were harvested and seeded in 96-well plates at a seeding density of 2×10^4 cells per well. CRM solutions were prepared at a concentration range of 25–300 μM and incubated for 2 and 24 h (h). Methanol without curcumin was used as a control. Ten microliter of MTT solution (5 mg/mL in PBS) was then added to each well and incubated for 4–5 h (37 °C, 5% CO_2) to allow MTT to be metabolized. The media was removed, and formazan (metabolic product of MTT) was re-suspended in 100 μL of DMSO and incubated for 1 h to enable thorough mixing of formazan into the solvent. Optical density was read at 560 nm using ELISA Plate Reader (Bio-Tek Instruments, Inc., Vermont, USA), and background was subtracted at 670 nm. The percent cell viability was measured from Eq. (1):

$$\text{Cell viability } (\%) = \frac{\text{Signal-background}}{\text{Blank-background}} \times 100. \quad (1)$$

2.2.4. Stability study in HBSS

The test was carried out by keeping the CRM solution in HBSS at four different pH values (5.5, 6.0, 6.5 and 7.4) in a shaker bath at 37 °C, 60 rpm and analyzing it after 1, 2 and 3 h. For pH 6.5, samples were also analyzed at 15, 30, 45, 60, 90 and 120 min. The concentration of CRM used was 170 μM. The stability test was also carried out in presence of lysed cells in order to assess the effect of intracellular enzymes on CRM degradation.

2.2.5. Permeability experiments

An initial stock solution of CRM in methanol was prepared. The stock solution was then diluted with HBSS to achieve a working concentration of 170 μM. The final concentration of methanol was 4% which is below 5% [18]. Some approaches to increase the solubility of CRM such as heat and alkali solubilization of CRM were carried out by Kurien et al. There was no heat disintegration of CRM, and the pharmacological activity of CRM was retained. Such systems can also be used to assess the permeability value of CRM [19,20].

Permeability experiments were performed in a shaker incubator (SW 23, Julabo, Seelbach, Germany) maintained at 37 °C and 60 rpm. Cells from passage number 37–50 were used for these experiments. The transepithelial electrical resistance (TEER) value was measured with a Millipore ERS voltameter (Millipore, Massachusetts, USA) in order to evaluate and determine the monolayer integrity. The TEER value was measured from the following Eq. (2):

$$\text{TEER} = (R_{\text{monolayer}} - R_{\text{blank}}) \times \text{A} \quad (2)$$

where $R_{\text{monolayer}}$ is the resistance of the cell monolayer along with the filter membrane, R_{blank} is the resistance of the filter membrane and A is the surface area of the membrane (0.7 cm^2 in 24-well plates).

Prior to the permeability assay, the cell monolayer was washed twice with PBS (pH 7.4) to remove traces of DMEM. After washing, the plates were incubated with transport buffer (HBSS) for 60 min at 37 °C in CO_2 incubator and the TEER value of the monolayer was measured. The transport buffer was then removed gently by aspiration. For apical to basolateral transport studies (A → B), 400 μL of the drug solution of CRM (170 μM) as well as the markers (ANT and FSD, 100 μM each) in HBSS was added to apical (A) side and 800 μL of the blank transport buffer was added to the basolateral (B) side. The basolateral to apical transport studies (B → A) were also carried out by adding CRM solution to the receiver compartment (B) followed by measuring concentration in the donor compartment (A). The permeability studies for pure CRM were conducted at pH 6.5 (A) and 7.4 (B) as well as in the presence of verapamil (100 μM) which is a P-gp inhibitor. Transport studies were also conducted on 1α, 25-$(OH)_2$ vitamin D_3-treated cell monolayers using itraconazole (100 μM) as a CYP 3A4 inhibitor. A sample volume of 700 μL was withdrawn from the respective compartment (basolateral side) at 15, 30, 45, 60, 90, and

120 min, and the volume withdrawn was replaced with blank transport buffer each time. The apparent permeability coefficients, P_{app} (cm/s), for both A → B and B → A studies were calculated from the following Eq. (3):

$$P_{app} = (dQ/dt)/(C_0 \cdot A) \quad (3)$$

where dQ/dt is the cumulative transport rate (μM/min) defined as the slope obtained by linear regression of cumulative transported amount as a function of time (min), A is the surface area of the filters or inserts (0.7 cm^2 in 24-wells), C_0 is the initial concentration of the compounds on the donor side (μM).

The concentration of the transported drug was measured from A → B and B → A, i.e., P_{app} (AB) and P_{app} (BA), respectively, and the efflux ratio (ER) was calculated from the following Eq. (4):

$$ER = P_{app}(AB)/P_{app}(BA) \quad (4)$$

2.2.6. Monolayer integrity test

At the end of the experiment, the monolayer integrity test was done by analyzing the concentration of LY in the apical and basolateral compartments. An initial stock solution of LY (50 mM) was prepared and diluted to 100 μM working solution. Four hundred microliter of the 100 μM working solution of LY was added to the apical side of Caco-2 cell monolayer (in the wells in which drug transport study was performed), and 800 μL of HBSS buffer (pH 7.4) was added to the basolateral side. The plate was then kept in a shaker incubator at 37 °C and 60 rpm. After 120 min, 700 μL and 300 μL of the samples were withdrawn from the basolateral side and apical side, respectively. The samples were analyzed by fluorescence spectroscopy at an excitation wavelength (λ_{ex}) of 485 nm and emission wavelength (λ_{em}) of 535 nm using a Spectrofluorophotometer (RF-5301-PC, Shimadzu, Kyoto, Japan).

2.2.7. HPLC analysis

The CRM samples from the receiver compartment were analyzed using a reversed-phase Shimadzu HPLC system (Kyoto, Japan) equipped with a model series SPD-M20A photodiode array detector a gradient elution pump with degassing device DGU-$20A_5$, a cooling autosampler SIL-20AC, a column heater/cooler CTO-10A VP and a system controller CBM-20A. Separations were performed by isocratic elution at 35 °C using a C18 (250 mm × 4.6 mm, 5 μm) stationary phase. Data were acquired via Class VP data acquisition software, version 6.12 SP1. Mobile phases used constituted of acetonitrile: tetrahydrofuran (4:1) as the organic phase and 1% w/v citric acid monohydrate (pH 3.0) as the aqueous phase. The mobile phase (65% organic and 35% aqueous) was pumped isocratically at 1 mL/min. The elution time was 3.5 min, and the detection wavelength was 435 nm.

For ANT and FSD, the mobile phase used consisted of acetonitrile: methanol: ultra pure water (Elgameter-TCM-1, Reservoir-40 L, Reverse osmosis unit Prima, Elga, Buckinghamshire, England) adjusted to pH 3.0 with o-phosphoric acid in a ratio of 24:24:52. Both drugs were quantified simultaneously, and the retention time for ANT and FSD was 3.4 min and 5.1 min, respectively.

2.2.8. Confocal microscopy

Determination of localization of CRM in cells was carried out by the confocal laser scanning microscopy (Olympus Fluoview 1000, Olympus, Tokyo, Japan). Slides for analysis were prepared by fixing the CRM-loaded cells on slides and sealing the sample with cover slip. The fluorescence of CRM was detected at an emission range of 420–480 nm with the maximum florescence being at 458 nm. The fluorescence with time was also studied. This was achieved by loading the cells with the same amount of stock solution and analyzing the samples at 15, 30, 45, 60, 90 and 120 min.

2.2.9. Absorption and desorption studies

The cell suspension containing the Caco-2 cells was taken at a cell density of 75,000 cells/400 μL. To it, CRM solution (170 μM) was added and incubated for different time intervals. The cell suspension containing CRM was then centrifuged at 5500 G for 6 min, and supernatant was removed. The pellet was washed with PBS, and lysis solution was added. CRM accumulated in the cells was extracted with methanol and analyzed by HPLC. The experiment was done on cells of different passages (48 and 54) on different days. For desorption studies, CRM-loaded cells after an incubation period of 120 min were centrifuged. The pellet was washed and resuspended in PBS. At specific time intervals, the cell suspension was again centrifuged and supernatant was withdrawn and analyzed by HPLC.

2.2.10. Statistical analysis

Statistical significance for P_{app} values was compared using the paired t-test assuming equal variances (SigmaStat version 3.5, San Jose, California, USA). The test was considered to be statistically significant if $P < 0.05$.

3. Results

3.1. Cytotoxicity test of CRM

Viability of cells was directly measured using the MTT test to evaluate the cytotoxicity of CRM on Caco-2 cells. MTT is a yellow tetrazolium salt that is oxidized by the mitochondrial dehydrogenase in living cells to give a dark blue formazan product. Damaged or dead cells show reduced or no dehydrogenase activity. Cell viability value of less than 50% indicates reduced mitochondrial activity. A higher cell viability of >80% ensured that the CRM concentrations were non-toxic to the cells. The cytotoxic concentration at 50% cell viability or CC_{50} value was observed at 265 μM as shown (Fig. 1). The proposed working concentration of 170 μM displayed approximately 80.8% cell viability after 24-h incubation. After 2-h incubation, however, concentrations up to 180 μM did not have any effect on the cells.

3.2. Evaluation of Caco-2 cell monolayer

The permeability of CRM was determined using the Caco-2 cell model. The TEER values measured were employed as an integrity

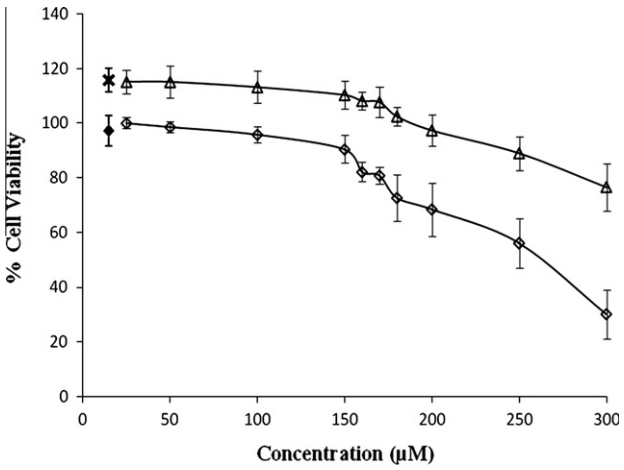

Fig. 1. Cytotoxicity results of CRM at different concentrations in Caco-2 cells using the MTT Assay. Incubation was done for CRM at 2 h (Δ), 24 h (◇) and for control samples at 2 h (×) and 24 h (♦). Values are represented as % cell viability ± SD for CRM at 2-h incubation ($n = 4$) and at 24-h incubation ($n = 8$).

evaluator of the monolayer formed. The TEER values for all wells were above 300 Ω cm^2 (n = 72).

The apparent permeability coefficient values were determined for the permeability markers FSD and ANT. FSD is a poorly permeable drug and showed a P_{app} value of $4.21 \times 10^{-6} \pm 0.07 \times 10^{-6}$ cm/s, whereas ANT which is a highly permeable drug showed a P_{app} value of $7.64 \times 10^{-5} \pm 0.7 \times 10^{-5}$ cm/s.

3.3. Stability of CRM in HBSS

The stability of CRM in HBSS was studied and expressed as the percentage of CRM remaining with time after incubation at 37 °C for 3 h. The stability of CRM was highest at pH 5.5 with 59.63% CRM remaining after 3 h (Fig. 2). The% CRM remaining decreased rapidly in the first two hours for all four pH conditions. Stability data indicated highest degradation of CRM at pH value of 7.4 which is commonly employed for the transport experiments.

3.4. Permeability studies

The Caco-2 cell model was used for studying the permeability of CRM. The permeability studies were carried out in a shaker bath kept at 60 rpm to prevent the influence of unstirred water layer [21]. The pH values for the apical side and basolateral side were 6.5 and 7.4, respectively. This was done keeping in mind the instability of CRM at pH 7.4 when compared to lower pH values. Furthermore, this condition has been optimized for Caco-2 transport studies [22]. The P_{app} values of the samples from A → B and B → A as well as in the presence of verapamil are shown (Fig. 3). CRM at pH 6.5 (A → B) showed the highest P_{app} value of $2.93 \times 10^{-6} \pm 0.94 \times 10^{-6}$ cm/s.

Contribution of active transport was investigated by performing the transport studies in the reverse direction, i.e., B → A. P_{app} values for the samples from A → B were significantly higher than the values obtained from B → A studies ($P < 0.05$). The efflux ratio was calculated as 0.967 ± 0.30. CRM did not show significant change ($P > 0.01$) in permeability in the presence of verapamil, a P-gp efflux inhibitor.

The monolayer integrity for permeability studies was confirmed by the transport of LY at the end of the experiment. The amount of LY that permeated was less than 2% after 6 h.

The recovery of the amount in the donor and receiver compartment was calculated at the end of the experiment and was expressed as a percentage of the amount added to the donor side at time zero (t_0). The recovery was calculated as follows:

$$\%\text{Recovery} = [(C_{R,120\text{min}} \cdot V_R + C_{D,120\text{min}} \cdot V_D)/(C_{D,0\text{min}} \cdot V_D)] \times 100 \quad (5)$$

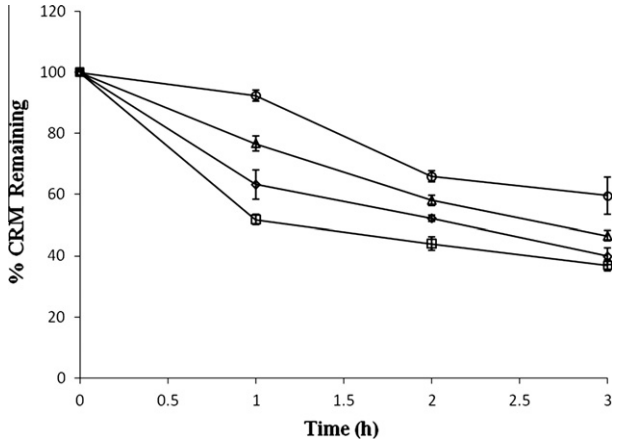

Fig. 2. Degradation of CRM in HBSS buffer at pH conditions 5.5 (○), 6.0 (Δ), 6.5 (◇) and 7.4 (□). Results are expressed as mean% CRM remaining with time ± SD (n = 3).

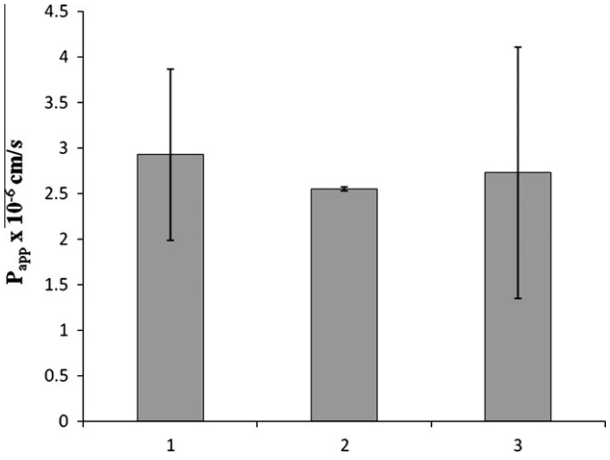

Fig. 3. Permeation studies of CRM (170 μM) showed the values of P_{app} ± SD (n = 4). 1 represents CRM at 6.5 respectively (A → B), 2 represents CRM at pH 6.5 (B → A) and 3 represents CRM with verapamil at pH 6.5 (A → B).

where $C_{R,120\text{min}}$ and $C_{D,120\text{min}}$ being the concentration measured after 120 min in the receiver and donor compartment, respectively. The% recovery of CRM at the end of the experiments was found to be 33.98 ± 4.21 at pH 6.5 (B → A) as given (Table 1).

The pH-dependent degradation of CRM in HBSS buffer has been shown in the preceding section. Another study was conducted to measure the percent of CRM degrading at the time points used for the transport experiments, i.e., at 15-min interval. The percent degradation with time was applied as a correction factor to assess the permeated and recovered amount of CRM concentration without the influence of degradation. This study aided in roughly estimating the permeability of CRM in the absence of its degradation. The P_{app} value obtained after considering the degradation of CRM in HBSS was $3.15 \times 10^{-6} \pm 1.08 \times 10^{-6}$ cm/s. The %recovery ± SD was calculated as 52.05 ± 6.44, and CRM loss was approximately 46%.

Incubation of CRM at pH 6.5 in presence of lysed cells displayed the combined effect of chemical stability and metabolism on CRM. Behavior of CRM at pH 6.5 with and without lysed cells is shown (Fig. 4). Approximately 12% more of CRM was lost in presence of lysed cells after 2 h of incubation.

3.5. Transport experiments in Caco-2 cell monolayer with CYP 3A4 expression

Transport studies on 1α, 25-$(OH)_2$ vitamin D_3-treated cell monolayers were compared with untreated cell monolayers (Fig. 5). CRM exposed to the treated cell monolayer showed the lowest P_{app} value of $1.93 \times 10^{-6} \pm 0.05 \times 10^{-6}$ cm/s. In presence of itraconazole, which is a CYP 3A4 inhibitor, and verapamil, a P-gp and CYP3A4 inhibitor, the P_{app} value for CRM increased to $3.52 \times 10^{-6} \pm 0.46 \times 10^{-6}$ cm/s.

3.6. CLSM microscopy and image analysis

Retention of CRM in cells was studied using CLSM. CRM at different concentrations showed different intensity of fluorescence

Table 1
Recovery of CRM at the end of the permeability experiments.

S. no.	CRM	% Recovery ± SD
1	At pH 6.5 (A → B)	33.98 ± 4.21
2	At pH 6.5 (B → A)	52.73 ± 2.98
3	At pH 6.5 with Verapamil	46.65 ± 5.23

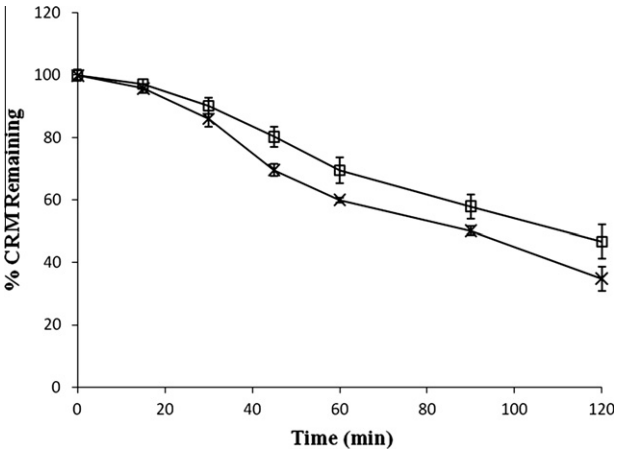

Fig. 4. The% CRM remaining with time at pH 6.5 (□) and at pH 6.5 in presence of lysed cells (x).

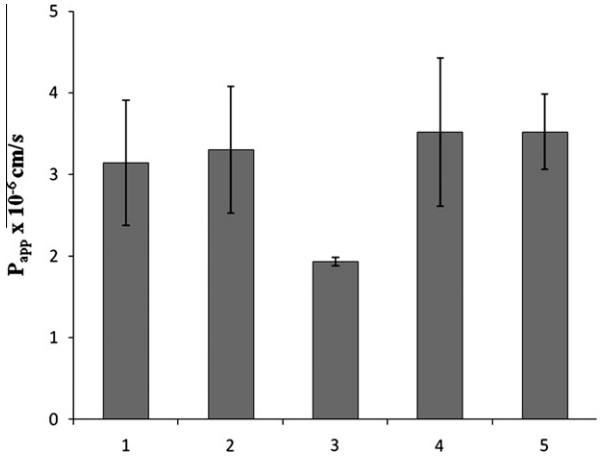

Fig. 5. P_{app} values for (1) CRM on untreated cell monolayer, (2) CRM with itraconazole on untreated cell monolayer, (3) CRM on 1α, 25-$(OH)_2$ vitamin D_3-treated cell monolayer, (4) CRM with itraconazole on 1α, 25-$(OH)_2$ vitamin D_3-treated cell monolayer, (5) CRM with itraconazole and verapamil on 1α, 25-$(OH)_2$ vitamin D_3 ($n = 3$).

after a 2-h incubation period (Fig. 6). The fluorescence intensity increased with time of exposure, indicating that the accumulation of CRM in the cells is also time dependent (Fig. 7).

3.7. Absorption and desorption studies

CLSM images qualitatively confirmed accumulation of CRM within the cells. Further quantitative assessment of absorption and desorption kinetics was carried out. The experiment was done at pH 3 to avoid any interference of degradation and at pH 6.5 to simulate the conditions of the transport experiments. More than 22% of CRM accumulated inside the cells after 2-h incubation at pH 6.5 (Table 2). The amount that was desorbed after 2 h was 9.93%. To assess the inter-day variation and the effect of passage number of cells, the experiment was performed in cells of two different passages on different days and the standard variation as taken.

The cumulative concentration of CRM with time for both absorption and desorption studies was plotted as shown (Fig. 8). It can be inferred from the graph that the rate of absorption of CRM inside the cells was significantly higher than the desorption rate. In both studies, irrespective of the pH, the absorption rates were higher.

4. Discussion

4.1. MTT Assay and evaluation of Caco-2 cell monolayer

The purpose of the MTT assay was to choose a concentration that would have no effect on cell viability during the course of the 2-h experimentation, the working concentration of 170 μM was evaluated to be safe, and this concentration was used for further studies. Moreover, after 24-h incubation, this concentration displayed cell viability above 80%. Previous reports also indicated that CRM at 30 μM concentration showed no cytotoxicity after 72-h incubation [23].

Monolayer integrity was controlled by ensuring a TEER value of >300 Ω cm^2. This assured that the Caco-2 cells had formed a proper monolayer with efficient tight junctions that allowed the passage of the compounds by the transcellular route. Another validation for monolayer formation was done by performing the permeability experiments for the two permeability markers ANT and FSD [16]. The P_{app} values of these compounds were comparable to the values already established in literature [22,24,25]. This further confirmed the validity of the protocol used for the monolayer formation.

4.2. Permeability studies

The Caco-2 permeability model system was used to determine the permeability of CRM. Gradient condition was maintained during the transport experiment. CRM displays three p*K*a values of 8.38 ± 0.04, 9.88 ± 0.02 and 10.51 ± 0.01 [26]. Since all the p*K*a values are much higher than the experimental pH values used, the ionization of CRM during the transport studies can be ruled out. According to the Caco-2 cell assay, model drugs having experimental P_{app} values of 14.0×10^{-6} cm/s are highly permeable whereas P_{app} values lesser than 5.0×10^{-6} cm/s are characteristic for low permeability model drugs [18]. Based on these values, it can be concluded that CRM is poorly permeable through the Caco-2 cell monolayer. In a previous study involving the permeability of CRM by the everted gut sac technique, insignificant transport and modification of CRM during the studies were reported. We further investigated the reasons for the low P_{app} value of CRM.

The results obtained showed that CRM exhibited a higher permeability value in the A → B direction when compared to B → A direction, indicating that CRM is not likely a substrate for active transport. Additionally, transport in presence of verapamil, a known P-gp inhibitor, gave similar P_{app} values when compared to CRM. These findings ruled out the possibility of efflux mechanism by P-gp in transport of CRM. However, the Caco-2 cell line does not express all the transporters and enzymes to a significant extent [27]; therefore, the role of other active transporters cannot be ruled out.

Recovery of CRM was calculated at the end of the experiments. Significant amount of CRM was lost during the experiments since only a small concentration of CRM (<2 μM) permeated. Mass balance studies defined as the ratio of the cumulative amount of CRM transported and remaining in the donor compartment, in relation to the initial amount in the donor compartment, showed that CRM had undergone drastic modifications during absorption. Possible contributors could be degradation of CRM in HBSS buffer, metabolism of CRM and accumulation of CRM in the cell wall. The permeated and recovered amount of CRM concentration was assessed without the influence of degradation. P_{app} did not alter significantly, thus signifying that excess of CRM was either metabolized or retained in cells. Caco-2 cells exhibit structural as well as functional differentiation patterns that are characteristic of human enterocytes. They express digestive enzymes like peptidases and disaccharidases. The differentiated cells also express xenobiotic-metabolizing enzymes including CYP 1A1,

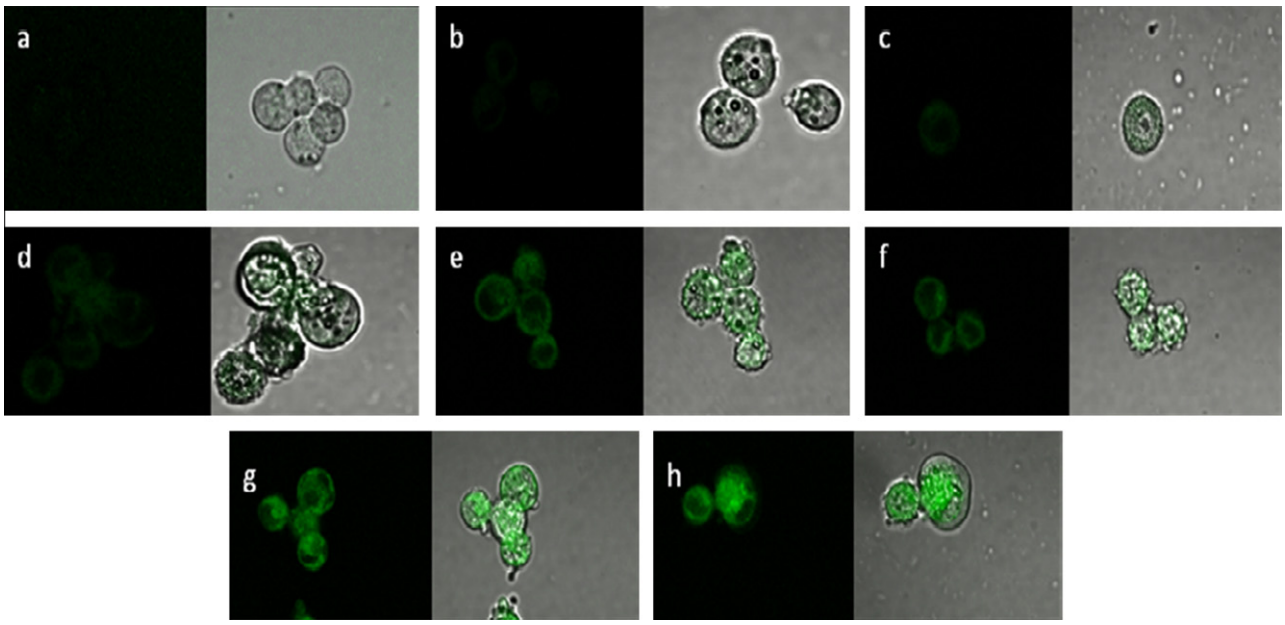

Fig. 6. Confocal micrographs (40×) of Caco-2 cells after incubation with CRM at different concentrations ranging from (a) Control (Caco-2 cells without CRM), (b) 25 μM, (c) 50 μM, (d) 100 μM, (e) 150 μM, (f) 170 μM, (g) 200 μM and (h) 256 μM. The left side shows fluorescence of CRM in laser beam and the right side shows phase-contrast images. (For interpretation of the references to colour in this figure legend, the reader is referred to the web version of this article.)

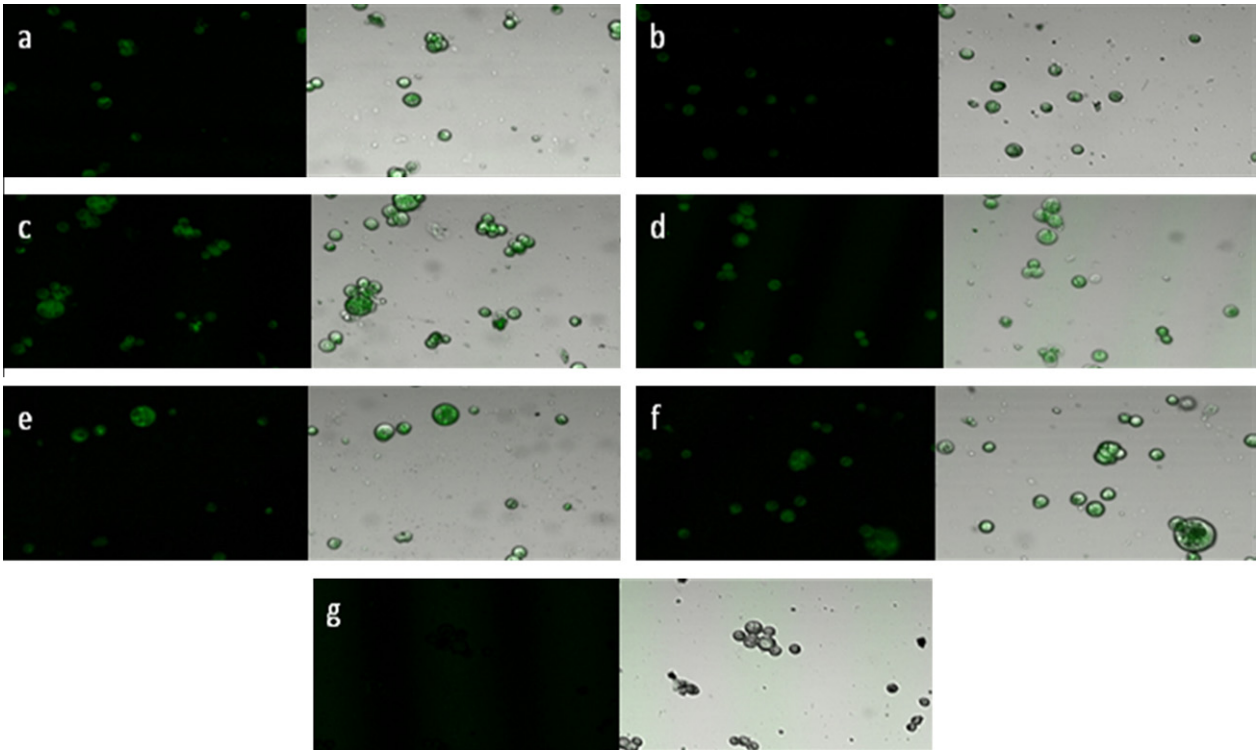

Fig. 7. Confocal micrographs (10×) of Caco-2 cells after incubation with CRM (170 μM) at different time intervals ranging from (a) 15 min, (b) 30 min, (c) 45 min, (d) 60 min, (e) 90 min, (f) 120 min, and (g) control cells. The left side shows fluorescence of CRM in laser beam and the right side shows phase-contrast images. (For interpretation of the references to colour in this figure legend, the reader is referred to the web version of this article.)

UDP-glucuronosyltransferases, phenol-sulfotransferases and glutathione-S-transferases [28]. Some of these enzymes may be responsible for CRM metabolism. CRM is reportedly sulfated by human phenol sulfotransferase isoenzymes SULT 1A1 and SULT 1A3 [10]. The incubation of CRM in presence of lysed cells at pH 6.5 exposed the compound to chemical and enzymatic degradation simultaneously. Additional amount of CRM was lost in presence of lysed cells. This established the role of metabolism in loss of CRM.

4.3. Transport experiments in Caco-2 cell monolayer with CYP 3A4 expression

The contribution of metabolism in CRM loss was investigated further on Caco-2 cell monolayer to investigate the role of enzymes such as CYP 3A4. Caco-2 cell monolayer is known to under-express CYP P450 isoforms. Treatment of Caco-2 cells with 1α, 25-$(OH)_2$ vitamin D_3, beginning at confluence, results in an increase in CYP

Table 2
Percentage of CRM that was absorbed and desorbed after 120 min ($n = 6$).

S. no.	Study	% Accumulated ± SD		Average reaction rate	
		pH 3	pH 6.5	pH 3	pH 6.5
1	Absorption	31.36 ± 1.05	22.57 ± 2.83	0.50	0.33
2	Desorption	14.41 ± 2.29	09.93 ± 2.80	0.33	0.15

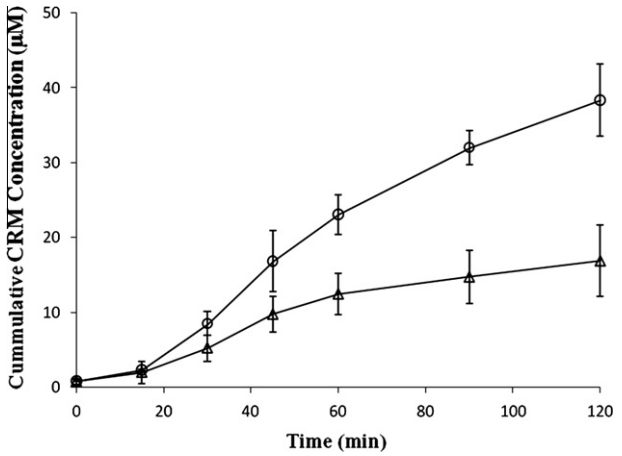

Fig. 8. Cumulative concentration of CRM with time for both absorption (○) and desorption (Δ) studies for pH 6.5.

3A4 mRNA expression with little effect on expression of other CYP isoforms such as CYP 3A5 or CYP 3A7. This treatment also increases NADPH cytochrome P450 reductase and P-gp [29,30]. The P_{app} value of CRM in treated cell monolayer was least when compared to P_{app} values of control group and CRM in presence of itraconazole and verapamil. These results supported our earlier evidence that metabolism has an effect on transport of CRM during intestinal absorption.

4.4. Absorption and desorption studies

Qualitative assessment of fluorescence intensity revealed that CRM exhibited concentration-dependent retention in cells with higher concentrations displaying greater fluorescence. The fluorescence intensity was also time dependent. Retention of CRM in cells can be correlated to its lipophilicity, depicted by a high log *P* value (3.29) [31]. The absorption and desorption kinetics of CRM in cells was quantitated. Compared to alkaline pH, the rate of absorption and desorption was higher in acidic conditions. For both pH conditions (3 and 6.5), reactions followed first-order kinetics and were concentration dependent up to the final time point used.

Accumulation of CRM within cells can explain the achievement of therapeutic benefits of CRM even when detectable concentration in blood plasma is not present. For instance, although CRM is not absorbed efficiently, it has been employed in the treatment of colorectal cancer since it is predominantly distributed in the colon [32]. It has also been proposed that CRM containing two electrophilic α, β unsaturated ketones can bind covalently with the thiol (SH) groups of cysteine residues of different proteins [33]. This particular reaction has been responsible for inducing the formation of topo II-DNA complexes by CRM [34,35]. Another group demonstrated that heat-solubilized CRM, which is solubility-enhanced CRM, binds to proteins and inhibits antigen–antibody interactions in *in vitro* studies [36]. This ability of CRM to bind to protein components correlates well with our findings where in the concentration of CRM absorbed in cells is much higher than that which is desorbed.

5. Conclusion

In the current study, we evaluated the permeability of CRM in Caco-2 cell monolayers, a validated model that imparts information on the absorption of drug compounds from the gut lumen. CRM was found to be poorly permeable across the Caco-2 cell monolayer. Coupled with literature reports of its poor aqueous solubility, these studies classified CRM as a BCS Class IV molecule. P-gp efflux did not play any role in the permeability of CRM. The reasons for the poor permeability of CRM were evaluated. The major factors that hampered its transport across the Caco-2 cell model included degradation in HBSS buffer, metabolism and accumulation within the cells. The stability profile of CRM in HBSS showed that approximately 52% of CRM remained after 2 h. Accumulation of CRM in cells was another major cause behind the low concentration of CRM transported, with approximately 22% of CRM retaining in cells. The amount of CRM that was desorbed back was relatively lesser than the amount that was absorbed. The difference in concentration was probably due to metabolism of CRM in cells and chemical degradation. Metabolism displayed a minor contribution when compared to the other two factors. Identification of these hurdles during the transport through the cell monolayer provides insight in designing the oral dosage forms for CRM. The issues that affect the CRM molecule such as stability, permeability and cell accumulation need to be addressed when formulating CRM in oral drug delivery systems.

Acknowledgements

Authors would like to thank Dr. Satyam K. Agrawal, scientist, Centre for Pharmaceutical Nanotechnology, National Institute of Pharmaceutical Education and Research for his technical support in CLSM analysis.

Yogesh B. Pawar acknowledges Department of Science and Technology (DST), Govt. of India for providing Senior Research Fellowship.

References

[1] G.K. Jayaprakasha, L. Jagan Mohan Rao, K.K. Sakariah, Chemistry and biological activities of *C. longa*, Trends Food Sci. Technol. 16 (12) (2005) 533–548.
[2] V. Lampe, J. Milobedzka, Studien über curcumin, Ber. Dtsch. Chem. Ges. 46 (1913) 2235–2240.
[3] A. Goel, A.B. Kunnumakkara, B.B. Aggarwal, Curcumin as "Curecumin": from kitchen to clinic, Biochem. Pharmacol. 75 (4) (2008) 787–809.
[4] K.Y. Yang, Oral bioavailability of curcumin in rat and the herbal analysis from *Curcuma longa* by LC–MS/MS, J. Chromatogr. B 853 (2007) 183–189.
[5] R.A. Sharma, S.A. Euden, S.L. Platton, D.N. Cooke, A. Shafayat, H.R. Hewitt, T.H. Marczylo, B. Morgan, D. Hemingway, S.M. Plummer, M. Pirmohamed, A.J. Gescher, W.P. Steward, Phase I clinical trial of oral curcumin: biomarkers of systemic activity and compliance, Clin. Cancer Res. 10 (20) (2004) 6847–6854.
[6] H.H. Tonnesen, M. Masson, T. Loftsson, Studies of curcumin and curcuminoids. XXVII. Cyclodextrin complexation: solubility, chemical and photochemical stability, Int. J. Pharm. 244 (1–2) (2002) 127–135.
[7] B.B. Aggarwal, A. Kumar, M.S. Aggarwal, S. Shishodia, Curcumin derived from turmeric (Curcuma longa): a spice for all seasons, in: D. Bagchi, H.G. Preuss (Eds.), Phytochemicals in Cancer Chemoprevention, CRC Press, Boca Raton, FL, 2004, pp. 349–387.
[8] C. Lao, M. Ruffin, D. Normolle, D. Heath, S. Murray, J. Bailey, M. Boggs, J. Crowell, C. Rock, D. Brenner, Dose escalation of a curcuminoid formulation, BMC Complement Altern. Med. 6 (1) (2006) 10.
[9] G. Garcea, D.J. Jones, R. Singh, A.R. Dennison, P.B. Farmer, R.A. Sharma, W.P. Steward, A.J. Gescher, D.P. Berry, Detection of curcumin and its metabolites in hepatic tissue and portal blood of patients following oral administration, Br. J Cancer. 90 (5) (2004) 1011–1015.
[10] C.R. Ireson, D.J.L. Jones, S. Orr, M.W.H. Coughtrie, D.J. Boocock, M.L. Williams, P.B. Farmer, W.P. Steward, A.J. Gescher, Metabolism of the cancer chemopreventive agent curcumin in human and rat intestine, Cancer Epidemiol. Biomarkers Prev. 11 (1) (2002) 105–111.
[11] A. Asai, T. Miyazawa, Occurrence of orally administered curcuminoid as glucuronide and glucuronide/sulfate conjugates in rat plasma, Life Sci. 67 (23) (2000) 2785–2793.
[12] C. Ireson, S. Orr, D.J.L. Jones, R. Verschoyle, C.-K. Lim, J.-L. Luo, L. Howells, S. Plummer, R. Jukes, M. Williams, W.P. Steward, A. Gescher, Characterization of

metabolites of the chemopreventive agent curcumin in human and rat hepatocytes and in the rat in *vivo*, and evaluation of their ability to inhibit phorbol ester-induced prostaglandin E2 production, Cancer Res. 61 (3) (2001) 1058–1064.
[13] Y.-J. Wang, M.-H. Pan, A.-L. Cheng, L.-I. Lin, Y.-S. Ho, C.-Y. Hsieh, J.-K. Lin, Stability of curcumin in buffer solutions and characterization of its degradation products, J. Pharm. Biomed. Anal. 15 (1996) 1867–1876.
[14] H.H. Tonnesen, J. Karlsen, Studies on curcumin and curcuminoids. VI. Kinetics of curcumin degradation in aqueous solution, Z. Lebensm. Unters. Forsch. 180 (5) (1985) 402–404.
[15] D. Suresh, K. Srinivasan, Studies on the *in vitro* absorption of spice principles – curcumin, capsaicin and piperine in rat intestines, Food Chem. Toxicol. 45 (8) (2007) 1437–1442.
[16] Center for Drug Evaluation and Research, Food and Drug Administration, Rockville, MD, Guidance for Industry. "Waiver of *In-vivo* Bioavailability and Bioequivalence Studies for Immediate-Release Solid Oral Dosage Forms Based on a Biopharmaceutics Classification System", 2000.
[17] X.-L. Hou, K. Takahashi, N. Kinoshita, F. Qiu, K. Tanaka, K. Komatsu, K. Takahashi, J. Azuma, Possible inhibitory mechanism of Curcuma drugs on CYP3A4 in 1[alpha], 25 dihydroxyvitamin D3 treated Caco-2 cells, Int. J. Pharm. 337 (1–2) (2007) 169–177.
[18] D.A. Volpe, P.J. Faustino, A.B. Ciavarella, E.B. Asafu-Adjaye, C.D. Ellison, L.X. Yu, A.S. Hussain, Classification of drug permeability with a Caco-2 cell monolayer assay, Clin. Res. Reg. Affairs 24 (1) (2007) 39–47.
[19] B.T. Kurien, A. Singh, H. Matsumoto, R.H. Scofield, Improving the solubility and pharmacological efficacy of curcumin by heat treatment, Assay Drug Dev. Technol. 5 (4) (2007) 567–576.
[20] B.T. Kurien, R.H. Scofield, Curcumin/turmeric solubilized in sodium hydroxide inhibits HNE protein modification – an *in vitro* study, J. Ethnopharmacol. 110 (2) (2007) 368–373.
[21] K.A. Youdim, A. Avdeef, N.J. Abbott, *In vitro* trans-monolayer permeability calculations: often forgotten assumptions, Drug Discov. Today 8 (21) (2003) 997–1003.
[22] S. Yamashita, T. Furubayashib, M. Kataokaa, T. Sakanea, H. Sezaki, H. Tokuda, Optimized conditions for prediction of intestinal drug permeability using Caco-2 cells, Eur. J. Pharm. Sci. 10 (2000) 195–204.
[23] X.-L. Hou, K. Takahashi, K. Tanaka, K. Tougou, F. Qiu, K. Komatsu, K. Takahashi, J. Azuma, Curcuma drugs and curcumin regulate the expression and function of P-gp in Caco-2 cells in completely opposite ways, Int. J. Pharm. 358 (1–2) (2008) 224–229.
[24] M. Uchida, T. Fukazawa, Y. Yamazaki, H. Hashimoto, Y. Miyamoto, A modified fast (4 day) 96-well plate Caco-2 permeability assay, J. Pharmacol. Toxicol. Methods 59 (1) (2009) 39–43.
[25] T. Korjamo, P. Honkakoski, M.R. Toppinen, S. Niva, M. Reinisalo, J.J. Palmgren, J. Monkkonen, Absorption properties and P-glycoprotein activity of modified Caco-2 cell lines, Eur. J. Pharm. Sci. 26 (3–4) (2005) 266–279.
[26] M. Bernabe-Pineda, M.T. Ramirez-Silva, M. Romero-Romo, E. Gonzalez-Vergara, A. Rojas-Hernandez, Determination of acidity constants of curcumin in aqueous solution and apparent rate constant of its decomposition, Spectrochim. Acta A Mol. Biomol. Spectrosc. 60 (2004) 1091–1097.
[27] N. Maubon, M. Le Vee, L. Fossati, M. Audry, E. Le Ferrec, S. Bolze, O. Fardel, Analysis of drug transporter expression in human intestinal Caco-2 cells by real-time PCR, Fundam. Clin. Pharmacol. 21 (6) (2007) 659–663.
[28] V. Meunier, M. Bourrie, Y. Berger, G. Fabre, The human intestinal epithelial cell line Caco-2; pharmacological and pharmacokinetic applications, Cell Biol. Toxicol. 11 (3–4) (1995) 187–194.
[29] P. Schmiedlin-Ren, K.E. Thummel, J.M. Fisher, M.F. Paine, K.S. Lown, P.B. Watkins, Expression of enzymatically active CYP3A4 by Caco-2 cells grown on extracellular matrix-coated permeable supports in the presence of 1alpha, 25-dihydroxyvitamin D3, Mol. Pharmacol. 51 (1997) 741–754.
[30] J.M. Fisher, S.A. Wrighton, P.B. Watkins, P. Schmiedlin-Ren, J.C. Calamia, D.D. Shen, K.L. Kunze, K.E. Thummel, First-pass midazolam metabolism catalyzed by 1alpha, 25-dihydroxy vitamin D3-modified Caco-2 cell monolayers, J. Pharmacol. Exp. Ther. 289 (2) (1999) 1134–1142.
[31] T.M.D. Mauro, Intranasally administering curcumin prodrugs to the brain to treat Alzheimer's disease, US Patent, US 2008/0076821 A1, 2008.
[32] J.J. Johnson, H. Mukhtar, Curcumin for chemoprevention of colon cancer, Cancer Lett. 255 (2) (2007) 170–181.
[33] M. Lopez-Lazaro, Anticancer and carcinogenic properties of curcumin: considerations for its clinical development as a cancer chemopreventive and chemotherapeutic agent, Mol. Nutr. Food Res. 52 (Suppl. 1) (2008) S103–S127.
[34] C. Martin-Cordero, M. Lopez-Lazaro, M. Galvez, M.J. Ayuso, Curcumin as a DNA topoisomerase II poison, J. Enzyme Inhib. Med. Chem. 18 (6) (2003) 505–509.
[35] H. Wang, Y. Mao, A.Y. Chen, N. Zhou, E.J. LaVoie, L.F. Liu, Stimulation of topoisomerase II-mediated DNA damage via a mechanism involving protein thiolation, Biochemistry 40 (11) (2001) 3316–3323.
[36] B.T. Kurien, A. D'Souza, R.H. Scofield, Heat-solubilized curry spice curcumin inhibits antibody–antigen interaction in *in vitro* studies: a possible therapy to alleviate autoimmune disorders, Mol. Nutr. Food Res. 54 (8) (2010) 1202–1209.